ACI MATERIALS JOURNAL TECHNICAL PAPER

Title no. 107-M53

# Numerical Simulation of Stress Waves on Surface of Strongly Heterogeneous Media

by Dimitrios G. Aggelis

*In this paper, the propagation of stress waves in a strongly heterogeneous medium is examined numerically. Low-density inclusions are used to model cracks in a stiff matrix. The volume content of inclusions affects, to a great extent, the shape and the velocity of the propagating wave. Additionally, the pattern and orientation of the simulated cracks relative to the propagation direction influences the individual wave modes (longitudinal and Rayleigh) in different ways. The aim of this study is to shed light on surface-wave propagation in damaged cementitious materials to establish new features similar to or more sensitive than longitudinal velocity for damage characterization.*

**Keywords:** damage assessment; longitudinal wave; nondestructive testing; simulation; surface wave; velocity.

## INTRODUCTION

Stress-wave propagation methods are commonly used for damage characterization in concrete. In some cases, when specific macroscopic defects are targeted (for example, delaminations, ungrouted tendon ducts, and surface breaking cracks), methods based on stress waves provide accurate information for characterizing the defect. In other cases, however, when there is distributed cracking, results are only qualitative due to inherent difficulties resulting from material inhomogeneity and attenuation.[1] Reliable characterizations rely on an understanding of wave propagation in inhomogeneous media. Therefore, combined studies involving experiments and numerical simulations are essential. In recent experimental studies, wave propagation parameters such as velocity and attenuation have been correlated with the typical shape and content of cracks.[2-6] Theoretical solutions by multiple scattering theory yield satisfactory explanations when spherical inhomogeneities are assumed.[5,7-9] However, the shapes of inhomogeneities influence wave propagation parameters, such as velocity and attenuation, and should be taken into account.[10] The effect of the actual shapes of cracks has not been adequately theoretically addressed, especially for the case of surface waves in a medium with random patterns of inhomogeneities. In literature, numerical simulations have been conducted for different cases of wave propagation in concrete, for example, for acoustic emission signals propagating through tendon ducts or surface waves influenced by reinforcing bars.[11,12] The benefit of simulations is that they enhance our understanding of wave propagation in the sense of what behavior should be expected for different conditions. Additionally, many different cases can be studied more efficiently than by experimental methods.[13]

Previous studies by the author[2-4] involved mortar with small vinyl plate inclusions (15 x 15 x 0.2 mm [0.59 x 0.59 x 0.008 in.]) simulating microcracks at different concentrations, that is, 0, 1, 5, and 10% by volume. In these studies,[2-4] the water-cement ratio (*w*/*c*) and sand-cement ratio by mass were 0.5 and 2, respectively; and the maximum aggregate size was 3 mm (0.12 in.) (too small compared with the vinyl inclusions). The vinyl inclusions were added after the other ingredients were mixed. The mortar with the vinyl inclusions was mixed for another 2 minutes and was then placed in the forms. The specimens (cubes of 150 mm [5.9 in.] side) were cured in water for 28 days and measurements of longitudinal and Rayleigh wave velocities were conducted after several days of air drying. It was found that Rayleigh waves are influenced much more by inhomogeneities—in terms of velocity and dispersion—than longitudinal waves.[3] Additionally, the experimental variability of different measurements on the same specimen was close to zero for sound mortar but was raised to approximately 20% for high "cracking" content, implying a strong influence of localized heterogeneity. Although the total number of inclusions makes up a specific volume content of the whole specimen, it is possible that the specific volume examined between two sensors contains fewer or more inclusions. Therefore, one measurement might not be representative. This is why a large number of measurements on several specimens should be done and their statistical scatter examined.

The aforementioned outcomes deserve detailed numerical studies because the classical elastic approach usually employed for cementitious materials cannot provide reasonable answers concerning the different influences of cracking on the various wave modes and the dependence of experimental scatter on crack density. Additionally, the actual shape of cracks cannot be addressed by "effective medium" approaches like multiple scattering theories[7,14] because analytical solutions exist only for spherical scatterers. The purpose of this paper is to present the results of numerical simulations for comparison with recent experimental surface wave studies in mortar with artificial cracks[3,4] to propose new sensitive parameters for material characterization.

## RESEARCH SIGNIFICANCE

New methods are highly sought for nondestructive testing of large concrete surfaces. Using the same equipment as for pulse velocity measurements, other wave propagation parameters can be exploited that are more sensitive to damage, as discussed herein. The combined study of experimental and numerical results offers a better understanding of the mechanics of wave propagation through a damaged medium. Modeling the actual shape of cracks yields more realistic conclusions than the previously used spherical inclusions. Rayleigh wave velocity, the ratio of Rayleigh to longitu-

*ACI Materials Journal*, V. 107, No. 5, September-October 2010.
MS No. M-2009-012.R2 received November 6, 2009, and reviewed under Institute publication policies.  Pertinent discussion including authors' closure, if any, will be published in the July-August 2011 *ACI Materials Journal* if the discussion is received by April 1, 2011.

**Dimitrios G. Aggelis** *is an Assistant Professor in the Materials Science and Engineering Department at the University of Ioannina, Ioannina, Greece. He received his diploma in mechanical engineering and his PhD in nondestructive testing of concrete from the University of Patras, Patras, Greece. He has worked as a research fellow at the Tobishima Research Institute of Technology, Chiba, Japan. His research interests include concrete damage characterization using nondestructive testing techniques.*

**Table 1—Properties of materials used in numerical model**

| | λ, GPa (ksi) | μ, GPa (ksi) | *E*, GPa (ksi) | ν | ρ, kg/m$^3$ (lb/ft$^3$) | $C_P$, m/s (ft/s) | $C_R$, m/s (ft/s) | $C_R/C_P$ |
|---|---|---|---|---|---|---|---|---|
| Mortar matrix | 9.0 (1305) | 13.0 (1885) | 31.3 (4496) | 0.20 | 2160 (135) | 4025 (13,205) | 2239 (7346) | 0.556 |
| Inclusions | 1.7 (247) | 1.15 (167) | 3.0 (435) | 0.30 | 1200 (75) | 1826 (5991) | 908 (2979) | 0.497 |
| Effective* | 7.77 (1127) | 11.01 (1597) | 26.6 (3858) | 0.207 | 2064 (129) | 3800 (12,467) | 2108 (6916) | 0.555 |

*Properties as calculated by Christensen model[19] for 10% volume of inclusions in matrix.

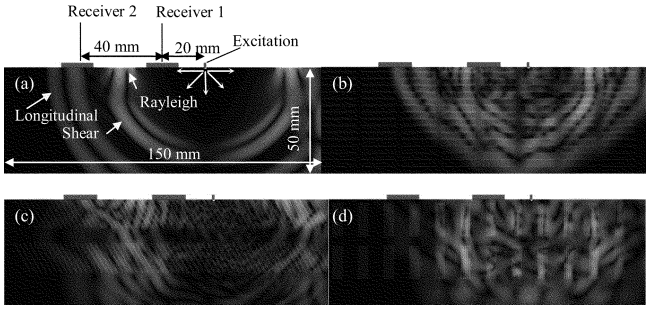


*Fig. 1—Geometry of numerical model and snapshot of displacement field 15 μs after excitation for: (a) plain mortar and mortar with vinyl inclusions of different patterns; (b) horizontal; (c) inclined by 60 degrees; and (d) vertical bunches. Total content of inclusions is 5% for (b), (c), and (d).*

dinal velocity, and the experimental scatter of the measurements are affected by the amount and orientation of cracks.

## NUMERICAL MODEL

The fundamental equation governing the two-dimensional (2D) propagation of stress waves in a perfectly elastic medium, ignoring viscous losses is as follows

$$\rho\frac{\partial^2 u}{\partial t^2} = \mu\nabla^2 u + (\lambda+\mu)\nabla\nabla\cdot u \qquad (1)$$

where $u = u(x,y,t)$ is the time-varying displacement vector; ρ is the mass density; λ and μ are the first and second Lamé constants, respectively; and $t$ is time. The focus is on simulating the same cases examined experimentally. Certain prerequisites should be followed, however, so that the analysis leads to reliable results. The simulations were conducted with commercially available software[15] that solves the previous equation using the finite difference method in the plane strain case. Equation (1) is solved with respect to the boundary conditions of the model, which include the input source that has predefined time-dependent displacements at a given location and a set of initial conditions.[16] For heterogeneous media like the one studied herein, wave propagation in each distinct homogeneous phase (in this case, mortar matrix and inclusions) is solved according to Eq. (1), whereas the continuity conditions for stresses and strains must be satisfied on the interfaces.[16]

Materials were considered elastic without viscosity components. Mechanical properties were set similar to the experimental material properties.[2] The numerical model included the mortar matrix with Lamé constants λ = 9 GPa (1305 ksi) and μ = 13 GPa (1885 ksi) and a density of 2160 kg/m$^3$ (135 lb/ft$^3$). The corresponding properties of the inclusions were λ = 1.7 GPa (247 ksi) and μ = 1.15 GPa (167 ksi) and a density of 1200 kg/m$^3$ (75 lb/ft$^3$). These properties, as well as elastic moduli $E$, Poisson's ratio ν, longitudinal $C_P$, and Rayleigh wave velocities $C_R$, are included in Table 1. The low mechanical properties of the inclusions guaranteed a strong impedance mismatch and, therefore, strong scattering interactions.

The excitation used experimentally (pencil lead break)[3,4] contained a band of frequencies up to 200 kHz, with a center frequency at approximately 100 kHz. Therefore, the simulations were conducted using a displacement excitation of one cycle of 100 kHz, which contained a broad band of frequencies of approximately 100 kHz. Two "receivers" were placed on the surface of the specimen 20 and 60 mm (0.787 and 2.36 in.) away from the source, as shown in Fig. 1(a). The receivers provided the average vertical displacement over their length, meaning that the receiver signal represents the average response over a number of nodes. Considering the mesh resolution of 0.1 mm (0.004 in.) and a receiver surface of 15 mm (0.59 in.), the transient response recorded at each step is the average displacement of 150 surface nodes. The snapshot of Fig. 1(a) shows the longitudinal and shear wavefronts spreading away from the point source, as well as the Rayleigh wave between the two receivers for material without the inclusions. It is noted that all of the results come from the vertical motion of the surface. The R-wave certainly has a vertical motion component, which is much stronger than the horizontal; therefore, it can be easily captured by the receiver on the surface. On the other hand, the L-wave has only a horizontal component. It can still be detected by the receiver, however, due to Poisson's ratio of the material, which induces a vertical displacement over the transient stress field.

Except for the case of solid mortar, three inclusion contents were used in the numerical models 1, 5, and 10% of the total area of the cross section. The shape of the inclusions was 15 x 0.2 mm (0.59 x 0.008 in.) for the 2D model while, as stated, the experimental inclusions were plates of 15 x 15 x 0.2 mm (0.59 x 0.59 x 0.008 in.).[2,3] For a fixed content and shape of the inclusions, there are infinite possible combinations of orientations and local concentration variations. Therefore, any specific pattern used for simulation will be one of a vast number of possible cases. In this study, several predefined arrangements of inclusions were used (for example, cases with all inclusions horizontal, cases with all inclusions vertical, or all inclined inclusions at a certain angle). In this way, it is possible to draw conclusions about how the orientation of the simulated cracks influences wave propagation. For each inclusion content, 12 patterns of orientations and local concentrations of inclusions were examined, as shown in Table 2. The patterns included: horizontal (parallel to the surface and the surface wave propagation direction), as seen in Fig. 1(b); vertical; inclined by ±30, ±45, and ±60 degrees (Fig. 1(c)); combinations of horizontal and vertical; and bunches of horizontal and vertical inclusions (Fig. 1(d)). The simulations were repeated after moving the positions of excitation and the receivers by 10 mm (0.394 in.) two times,

so that three waveforms were recorded for each inclusion pattern. Even if the total concentration of inclusions is constant, moving the excitation and receivers' positions resulted in different velocities. This was done to include the effect of sensor position relative to the underlying inhomogeneity and determine if the experimental variation observed in previous studies[3,4] was due to experimental uncertainties (for example, coupling conditions) or if it was due to the material inhomogeneity itself.

The model geometry was 150 x 50 mm (5.90 x 1.96 in.) and an infinite boundary condition was used at the bottom to avoid reflections. The element size (mesh) was 0.1 mm (0.004 in.). For a frequency of 100 kHz, the Rayleigh wavelength is calculated to be approximately 25 mm (0.98 in.) and the longitudinal wavelength approximately 40 mm (1.57 in.). This satisfies the requirement[15] of at least 10 to 20 nodes per wavelength and results in reasonable accuracy.[17] Figure 2(a) shows the waveforms at the two receiver positions for the case of plain mortar for a mesh size of 0.1 mm (0.004 in.). Figure 2(b) shows the transient waveforms obtained for a material with 10% vertical bunches of inclusions using the same mesh size and also a coarser mesh of 0.2 mm (0.008 in.). It is apparent that the waveforms are identical, and the longitudinal and Rayleigh wave velocities measured using the strong positive peaks were exactly the same for the two mesh sizes. This shows that the results converge even for a mesh size of 0.2 mm (0.008 in.), while in this study, a 0.1 mm (0.004 in.) mesh size was used. The time step was 0.01975 μs, meaning that for a frequency of 100 kHz (a period of 10 μs), more than 500 points were used in a cycle, ensuring adequate depiction.

## SIMULATION RESULTS

The longitudinal wave velocity is measured by the transit time ($\delta t_L$) of the first detectable disturbance of the wave between the receivers. The Rayleigh surface wave, on the other hand, carries most of the energy; therefore, its arrival is usually clear after the initial longitudinal wave arrivals. The reference point used for Rayleigh velocity calculation is taken as the first large peak of the Rayleigh wave signal.[3,4] The distance between the receivers divided by the delay time $\delta t_R$ (refer to Fig. 2) of the reference points yields the Rayleigh wave velocity.

Figure 3(a) shows the relation between wave velocity and inclusion content. For plain material, the longitudinal wave velocity is 4025 m/s (13,205 ft/s) as defined by the mechanical properties of the matrix used in the model. As the inclusion content increases up to 10%, the velocity decreases smoothly to 3370 m/s (11,050 ft/s) and is quite close to the experimental value.[3] For the Rayleigh wave velocity, it starts at 2240 m/s (7350 ft/s) for the plain material and is reduced to 1450 m/s (4750 ft/s) for the model with 10% inclusions, also closely following the experimental trend. The numerical results represent the average velocities of all of the different orientations of inclusions used in the models to simulate as closely as possible the actual experimental case where the orientation of the inclusions is considered random.[2,18]

By using different established models for the calculation of properties of composites based on the properties of the constituents[19,20] for 10% volume content of inclusions, the longitudinal velocity of the effective medium should be approximately 3800 m/s (12470 ft/s, Table 1). These models, however, only consider the volume content of the inclusions. The experimental and numerical results produced by using inclusions with a realistic crack shape show that velocity

**Table 2—Different patterns of inclusions used in simulation**

| | | | |
|---|---|---|---|
| Horizontal (0 degrees) uniformly distributed | 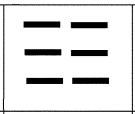 | Horizontal bunches | 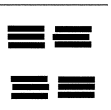 |
| Vertical (90 degrees) uniformly distributed |  | Vertical bunches |  |
| 30 |  | –30 |  |
| 45 |  | –45 |  |
| 60 |  | –60 |  |
| 0 and 90 degrees | 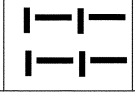 | Horizontal (0 degrees)* | 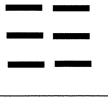 |

*First line of inclusion is on surface.

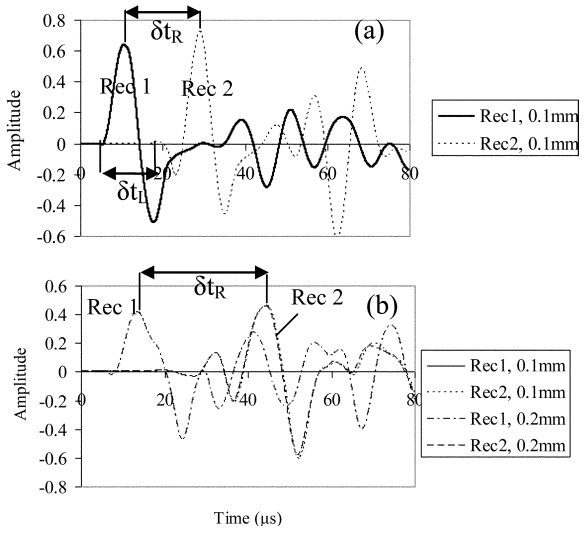


*Fig. 2—Transient waveforms of two receivers for: (a) plain material; and (b) material with vertical bunches of inclusions (10% of total area). Legend includes mesh size used for simulations.*

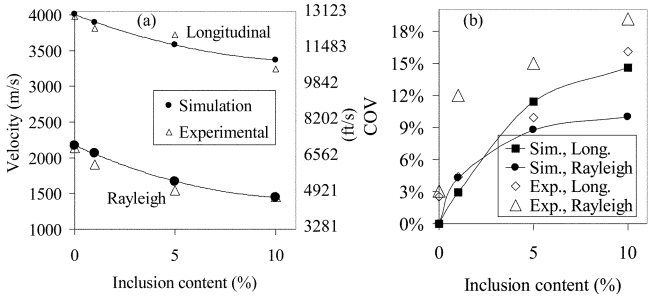


*Fig. 3—(a) Average wave velocity versus inclusion content; and (b) coefficient of variation of wave velocity versus inclusion content.*

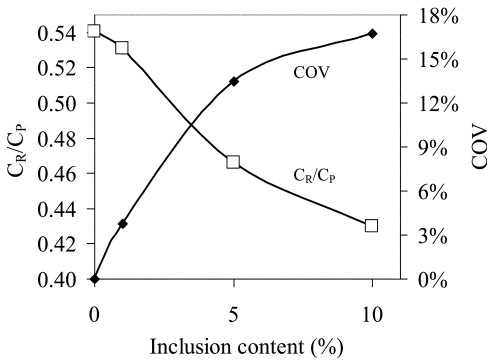


*Fig. 4—Ratio of Rayleigh to longitudinal wave velocity and COV versus inclusion content.*

decreases much more, being greatly affected also by the shape of the inclusions.

Simulations confirm that inhomogeneity affects Rayleigh waves more than longitudinal waves because for 10% inclusions, the reduction of Rayleigh wave speed is approximately double that of the longitudinal wave speed (35% and 16%, respectively). It is therefore implied that Rayleigh waves, which have displacement vectors in two directions, are more sensitive to the presence of inhomogeneity than longitudinal waves. The difference in the behaviors of different wave modes is not peculiar to heterogeneous materials,[3,4] as will be discussed in another section in more detail. The different behavior of Rayleigh and longitudinal waves has also been theoretically studied from the viewpoint of gradient elastic theories in materials with microstructure.[21]

As mentioned previously, three waveforms for each of the 12 inclusion patterns were produced after "sliding" the excitation-receiver array, making a total of 36 different simulated experiments for each inclusion content. The scatter in wave velocities for this population is also strongly dependent on the inclusion content. In Fig. 3(b), it is seen that the coefficient of variation ([COV], standard deviation divided by the average of the wave velocities) increases with the inclusion content. For the homogeneous plain mortar model, different excitation-receiver positions do not yield any variation. For just 1% of inclusions, the COV from the simulations rises to 3 to 4% for both wave types; at 10% inclusions, the COV reaches 15% and 10% for longitudinal and Rayleigh wave velocities, respectively. The experimental data showed a similar increasing trend except that the variation of Rayleigh wave speed was higher than the longitudinal wave speed for high inclusion content. The COV of 3% for the plain mortar (refer to Fig. 3(b)) can be attributed to experimental uncertainties (mainly coupling conditions) as well as local variations of mortar properties. For 10% of inclusions, the COV increases up to approximately 20%, showing that one single measurement could easily be misleading. As for the fact that the Rayleigh wave velocity exhibits a lower COV than the longitudinal velocity in the simulations, no explanation can be given. The use of COV as a damage indicator is quite new and needs more study, both by experiments and simulations. The significance lies in the fact that the COV of measured Rayleigh and longitudinal wave velocities increases monotonically with cracking and, therefore, can be used as an additional damage indicator.

## RELATION BETWEEN LONGITUDINAL AND RAYLEIGH WAVE VELOCITIES

For the value of Poisson's ratio ν of a typical cementitious material, which is approximately 0.2, the Rayleigh velocity $C_R$ is approximately 55% of the longitudinal velocity $C_P$.[22] When the material is deteriorated, its elastic modulus decreases. This means that both longitudinal and Rayleigh velocities decrease. Nominally, there is no effect on the ratio of longitudinal to Rayleigh velocities because the ratio depends only on Poisson's ratio ν[22]

$$C_P = \frac{1+\nu}{0.87+1.12\nu}\sqrt{\frac{2(1-\nu)}{(1-2\nu)}}C_R \quad (2)$$

The experimental results, however, showed that the ratio of Rayleigh to longitudinal velocities decreased from 0.55 (sound material) to 0.35 (material with 10% of inclusions).[3] The decrease is too great to be explained by a change of Poisson's ratio due the inclusions. In fact, to yield a ratio $C_R/C_P$ equal to 0.35, through Eq. (2), the Poisson's ratio should be higher than 0.4, which is not possible for cementitious material. Table 1 shows the computed Poisson's ratio for the effective material with 10% inclusions using the Christensen model.[19] Again, this model does not take into account the shape of the inclusions; thus, the resulted values are used just as a rule of thumb for the effective material's Poisson's ratio. The calculated value of 0.207 is nearly identical to the value of the matrix (0.2). Therefore, the change in the ratio of the velocities ($C_R/C_P$) is not attributed to a sharp increase in the Poisson's ratio to 0.4, a value which is excluded both by experience and composite materials model.

For the numerical simulations, the results for the ratio of Rayleigh to longitudinal wave velocity, $C_R/C_P$, are shown in Fig. 4. It is seen that for 0% of the inclusions, the ratio is at the expected level (0.54) defined by the elastic constants of plain mortar. The addition of the low density inclusions simulating cracks decreases this ratio, even for a content of 1%; whereas for 10% inclusions, the ratio is decreased to 0.43. This change represents a decrease of more than 20%, which indicates that this ratio is more sensitive to the presence of the inclusions than pulse velocity alone. For the experimental measurements, the decrease was even greater to a ratio of 0.35.

Simulations showed that the ratio $C_R/C_P$ is strongly influenced by the orientation of the inclusions. Examination of the results for individual patterns revealed that when the inclusions have a horizontal orientation, longitudinal wave velocity is hardly affected, even for the case of 10% inclusions measured at 3988 m/s (13,084 ft/s) compared with 4025 m/s (13,205 ft/s) for plain mortar. The Rayleigh wave velocity for the same horizontal orientation, however, showed a decrease to 1296 m/s (4252 ft/s) from 2239 m/s (7346 ft/s) for the plain mortar. In this case, $C_R/C_P = 0.32$. The case of 10% vertical inclusions yielded a lower longitudinal wave velocity (3620 m/s [11,877 ft/s]) than for horizontal inclusions but a higher Rayleigh wave velocity (1387 m/s [4551 ft/s]) with $C_R/C_P = 0.38$. For other orientations (for example, 60 degrees) this ratio was higher ($C_R/C_P = 0.52$). The sensitivity of $C_R/C_P$ to the orientation of simulated cracks may be attributed to the nature of the Rayleigh wave, which contains a vertical displacement vector that is stronger than the horizontal vector. From the aforementioned, it is seen that the concentration of "damage" is not the only parameter that influences wave propagation, because the crack orientation has a different effect on the individual wave modes. For nondestructive testing (NDT) of concrete, the change of velocity due to different orientations of cracks is crucial because quality estimation is commonly based solely on measured pulse

velocity. For a crack orientation that is conducive to propagation (for example, horizontal in this case), longitudinal wave velocity is not affected much, which gives a misleading characterization. However, the same cracks will have a greater influence on Rayleigh waves; therefore, combined measurements of different parameters are necessary for correct evaluation.

The statistical scatter of the parameter $C_R/C_P$ is also shown in Fig. 4. The COV increases from 0 for plain material up to 17% for high content of inclusions, which is greater than the scatter of velocities alone, as shown in Fig. 3(b).

It should be mentioned that the results presented previously concern the specific pulse introduced (one cycle of 100 kHz). It is highly likely that the values of the velocities would be somehow different for different excitation pulses. However, this pulse covers the usually applied frequencies in concrete, which is below 200 kHz.

## CONCLUSIONS

The characterization of microcracking in concrete structures based on stress wave propagation is a complicated task. This is because a number of parameters (amount of cracking, orientation, geometric pattern, and characteristic size of cracks) influence wave propagation behavior. Therefore, a relationship between a single wave feature and degree of cracking is difficult to establish. New features are sought that are more sensitive than pulse velocity but are as easy to measure. These new features may require that the whole ultrasonic waveform is acquired (as, for example, the identification of both Rayleigh and longitudinal modes, which cannot be conducted only by a simple threshold crossing algorithm). Waveform acquisition, however, is available in most of the contemporary pieces of equipment enabling the characterization of different modes as well as the amplitude of the waves. If this is not possible due to equipment limitations, examining the experimental scatter of a number of measurements will supply additional information on the severity of microcracking.

The most important conclusions of this combined experiment and numerical study are the following:

1. Rayleigh wave velocity is more sensitive to the existence of the inclusions that were used to simulate cracks, being reduced by approximately 35%, while longitudinal velocity decreases by approximately 15% for 10% volume of cracking.

2. The ratio of Rayleigh wave velocity to longitudinal wave velocity decreases very strongly (more than 20% when 10% volume of inclusions were present) due to the differential influence of microcracks on different wave modes.

3. The COV of wave velocities is close to zero for measurements on sound material and monotonically increases to 20% for 10% inclusions. The use of COV as another parameter to enhance the rough characterization offered by pulse velocity should be studied further.

4. Crack orientations that are "invisible" to P-wave measurements can be detected by Rayleigh waves.

5. The well-known elasticity relations between propagation velocities and elastic constants are derived for homogeneous and isotropic material. Concrete can be considered as such when undamaged. When numerous cracks are present, however, these relations do not provide predictions close to the experimental findings. Models including both distinct phases—like the numerical simulations of this study—seem more appropriate for the explanation of the behavior of damaged cementitious material.

6. The results of numerical simulations were close to experimental results. Because purely elastic materials were assumed in the models (neglecting viscous components), it is believed that elastic scattering is the main reason for the observed behavior. Simulations offer a valuable tool for studying a variety of cases that would be difficult or costly to reproduce by experiment.

Some of the next steps for the numerical simulation will be to use different shapes and sizes of the inclusions in the models (because the potential shapes are limitless), as well as to replace the low-density inclusions with actual cracks (zero density) to simulate actual damage in concrete. Additionally, the use of different frequencies should shed light on the strongly dispersive behavior observed experimentally.

## REFERENCES


1. Naik, T. R., and Malhotra, V. M., "The Ultrasonic Pulse Velocity Method," *CRC Handbook on Nondestructive Testing of Concrete*, V. M. Malhotra and N. J. Carino, eds., CRC Press, Boca Raton, FL, 1991, pp. 169-188.

2. Aggelis, D. G., and Shiotani, T., "Effect of Inhomogeneity Parameters on Wave Propagation in Cementitious Material," *ACI Materials Journal*, V. 105, No. 2, Mar.-Apr. 2007, pp. 187-193.

3. Aggelis, D. G., and Shiotani, T., "Experimental Study of Surface Wave Propagation in Strongly Heterogeneous Media," *Journal of the Acoustical Society of America*, V. 122, No. 5, 2007, pp. EL 151-157.

4. Aggelis, D. G., and Shiotani, T., "Surface Wave Dispersion in Cement-Based Media: Inclusion Size Effect," *NDT & E International*, V. 41, 2008, pp. 319-325.

5. Chaix, J. F.; Garnier, V.; and Corneloup, G., "Ultrasonic Wave Propagation in Heterogeneous Solid Media: Theoretical Analysis and Experimental Validation," *Ultrasonics*, V. 44, 2006, pp. 200-210.

6. van Wijk, K.; Komatitsch, D.; Scales, J. A.; and Tromp, J., "Analysis of Strong Scattering at the Micro-Scale," *Journal of the Acoustical Society of America*, V. 115, 2004, pp. 1006-1011.

7. Aggelis, D. G.; Tsinopoulos, S. V.; and Polyzos, D., "An Iterative Effective Medium Approximation (IEMA) for Wave Dispersion and Attenuation Predictions in Particulate Composites, Suspensions and Emulsions," *Journal of the Acoustical Society of America*, V. 116, No. 6, 2004, pp. 3443-3452.

8. Aggelis, D. G.; Polyzos, D.; and Philippidis, T. P., "Wave Dispersion and Attenuation in Fresh Mortar: Theoretical Predictions vs. Experimental Results," *Journal of the Mechanics and Physics of Solids*, V. 53, 2005, pp. 857-883.

9. Kim, J.-Y.; Ih, J.-G.; and Lee, B.-H., "Dispersion of Elastic Waves in Random Particulate Composites," *Journal of the Acoustical Society of America*, V. 97, 1995, pp. 1380-1388.

10. Kuster, G. T., and Toksoz, M. N., "Velocity and Attenuation of Seismic Waves in Two Phase Media: Part II—Experimental Results," *Geophysics*, V. 39, No. 5, 1974, pp. 607-618.

11. Schechinger, B., and Vogel, T., "Acoustic Emission for Monitoring a Reinforced Concrete Beam Subject to Four-Point-Bending," *Construction and Building Materials*, V. 21, 2007, pp. 483-490.

12. Wu T.-T.; Sun J.-H.; Tong J.-H., "On the Study of Elastic Wave Scattering and Rayleigh Wave Velocity Measurement of Concrete with Steel Bar," *NDT & E International*, V. 33, 2000, pp. 401-407.

13. Aggelis, D. G., "Numerical Simulation of Surface Wave Propagation in Material with Inhomogeneity: Inclusion Size Effect," *NDT & E International*, V. 42, 2009, pp. 558-563.

14. Biwa, S.; Ito, N.; Ohno, N., "Elastic Properties of Rubber Particles in Toughened PMMA : Ultrasonic and Micromechanical Evaluation," *Mechanics of Materials*, V. 33, 2001, pp. 717-728.

15. Wave2000, Cyber-Logic, Inc, NY (http://www.cyberlogic.org).

16. Kaufman, J. J.; Luo, G.; and Siffert, R. S., "Ultrasound Simulation in Bone," *IEEE Transactions on Ultrasonics, Ferroelectrics and Frequency Control*, V. 55, No. 6, 2008, pp. 1205-1218.

17. Moser, F.; Jacobs, L. J.; and Qu, J., "Modeling Elastic Wave Propagation in Waveguides with Finite Element Method," *NDT & E International*, V. 32, 1999, pp. 225-234.

18. Aggelis, D. G., and Momoki, S., "Numerical Simulation of Wave Propagation in Mortar with Inhomogeneities," *ACI Materials Journal*, V. 106, No. 1, Jan.-Feb. 2009, pp. 59-63.

19. Christensen, R. M., "A Critical Evaluation for a Class of Micromechanics Models," *Journal of the Mechanics and Physics of Solids*, V. 38, No. 3, 1990, pp. 379-404.

20. Budiansky, B., "On the Elastic Moduli of some Heterogeneous Materials," *Journal of the Mechanics and Physics of Solids*, V. 13, No. 4, 1965, pp. 223-227.

21. Georgiadis, H. G.; Vardoulakis, I.; and Velgaki, E. G., "Dispersive Rayleigh-Wave Propagation in Microstructured Solids Characterized by Dipolar Gradient Elasticity," *Journal of Elasticity*, V. 74, 2004, pp. 17-45.

22. Sansalone, M., and Carino, N. J., "Stress Wave Propagation Methods," *CRC Handbook on Nondestructive Testing of Concrete*, V. M. Malhotra, and N. J. Carino, eds., CRC Press, Boca Raton, FL, 1991, pp. 275-304.